Rev.Adv.Mater.Sci. 10 (2005) 362-366

STRUCTURAL AND MAGNETIC STUDY OF Mn_3O_4 NANOPARTICLES

América Vázquez-Olmos[1], Rocío Redón[1], M. Esther Mata-Zamora[1], Francisco Morales-Leal[2], Ana L. Fernández-Osorio[3] and José M. Saniger[1]

[1]Centro de Ciencias Aplicadas y Desarrollo Tecnologico, Cuautitlan-1, Universidad Nacional Autonoma de Mexico, Coyoacan, Mexico D. F., 04510, Mexico
[2]Instituto de Investigacion en Materiales, Cuautitlan-1, Universidad Nacional Autonoma de Mexico, Coyoacan, Mexico D. F., 04510, Mexico
[3]Facultad de Estudios Superiores, Cuautitlan-1, Universidad Nacional Autonoma de Mexico, Coyoacan, Mexico D. F., 04510, Mexico

Received: April 15, 2005

Abstract.A novel one step room temperature synthesis of nanocrystalline Mn_3O_4 hausmannite was carried out from a simple dissolution of manganese(II) acetate, in a mixture of N,N'-dimethylformamide (DMF) and water. Homogeneous nanocrystals like rods were obtained, with an average width and length of 6.6 ± 1.2 nm and 17.4 ± 4.1 nm respectively, and a preferential growth along the <001> direction. Magnetization measurements on a powdered sample showed a ferrimagnetic behavior at low temperature. The blocking temperature (T_B) was observed at 37K and the Curie temperature (T_C) at 40K.

1. INTRODUCTION

Mn_3O_4 has a normal spinel structure, the stable room temperature phase is tetragonal hausmannite (space group $I4_1/amd$ a = 5.726 Å, c = 9.470 Å) with Mn^{3+} and Mn^{2+} ions occupying the octahedral and tetrahedral positions of the spinel structure, respectively. The octahedral symmetry is tetragonally distorted due to Jahn-Teller effect on Mn^{3+} ions [1]. Mn_3O_4 is known to be an effective and inexpensive catalyst to limit the emission of NO_x and CO, which provides a powerful method to control air pollution. This material has also attracted interest as an active catalyst for the reduction of nitrobenzene or oxidation of methane. It has shown to be a corrosion-inhibiting pigment for epoxy-polyamide and epoxy-ester based primers and top coating. Moreover, Mn_3O_4 has been widely used as the main source of ferrite materials, which have applications in electronic and information technologies [2-6]. Nanometer sized Mn_3O_4, with notable increased surface area and greatly reduced size is expected to display better performance in these aspects of application.

In the last decade, solution chemical synthesis techniques such as the sol-gel process and the solvothermal method have been employed to prepare hausmannite nanoparticles, however these processes involve many reagents and require a post-treatment of heating at different temperatures [1,6-10].

In this sense, new synthesis methods that allow obtaining clean products are welcome, in particular when the final purpose is a technological application.

On the other hand, DMF as well as dimethyl sulfoxide (DMSO) have been proved to be very useful solvents in nanoparticle synthesis [11-16]. Their high dielectric constants allow charge separation;

Corresponding author: América Vázquez-Olmos, e-mail: amer@aleph.cinstrum.unam.mx

turning them into good solvents for ionic solids and polar or polarizable molecules.

Thus, herein we present a facile one step process at room temperature for the preparation of Mn_3O_4 nanoparticles and their structural and magnetic study.

2. EXPERIMENTAL

2.1. Materials

Manganese acetate tetrahydrated, $Mn(OAc)_2 \cdot 4H_2O$ (99% Aldrich), N,N'-dimethylformamide, DMF (99.8% Aldrich) and acetone, $CO(CH_3)_2$ (Fermont 99.7%) were purchased and used as received, without further purification. Ultra pure water (18 MΩ cm^{-1}) was obtained from a Barnsted E-pure deionization system.

2.2. Synthesis

0.03063 g of $Mn(OAc)_2 \cdot 4H_2O$, were dissolved in DMF (22.5 mL) under vigorous stirring. After this, 2.5 mL of ultra-pure water were added to get a final concentration of $5 \cdot 10^{-3}$M in 25 mL of DMF-H_2O (10%). The amber solution was stirred for further 30 minutes and the resulting solution left to stand for three months under normal conditions and the dark brown precipitate, was recovered by centrifugation (16000 rpm x 10 min), and washed first with water and then with acetone.

2.3. Instruments

UV-visible absorption spectra, (colloidal dispersion and powder) were obtained with an Ocean Optics USB2000 miniature fiber optic spectrometer. The Fourier transformed infrared (FTIR) was performed with a Nicolet Nexus 670 FT-IR infrared spectrometer from 4000 to 400 cm^{-1} with a resolution of 4 cm^{-1}, in a KBr wafer. X-ray diffraction pattern was measured in a D5000 Siemens equipment using Cu Kα radiation (λ=1.5406 Å). Transmission electron microphotographs (TEM) were obtained with a JEOL 1200EXII instrument, operating at 60 kV. A drop of the colloidal dispersion of Mn_3O_4 was deposited onto a 200 mesh Cu grids coated with a carbon/collodion layer. High-resolution transmission electron microphotographs (HR-TEM) were obtained with a JEOL 2000F instrument, operating at 200 kV, using the same sample preparation as in TEM. The particle size distribution was determined from digitalized amplified micrographs by averaging the larger and smaller axis diameter measured in each particle.

Magnetic measurements were performed on a SQUID Quantum Design magnetometer, on powdered samples of Mn_3O_4 nanoparticles. The temperature was varied between 2 and 300K according to a zero field cooling (ZFC) / Field cooling (FC) procedure at 100 Oe, and the hysteresis loop was obtained at 5K, in a magnetic field of up to ± 3 T.

3. RESULTS AND DISCUSSION

3.1 Structural study

The colloidal dispersion of Mn_3O_4 was monitored by UV-visible electronic absorption spectroscopy, as shown in Fig. 1. At the beginning the UV-visible spectrum of a freshly prepared solution of

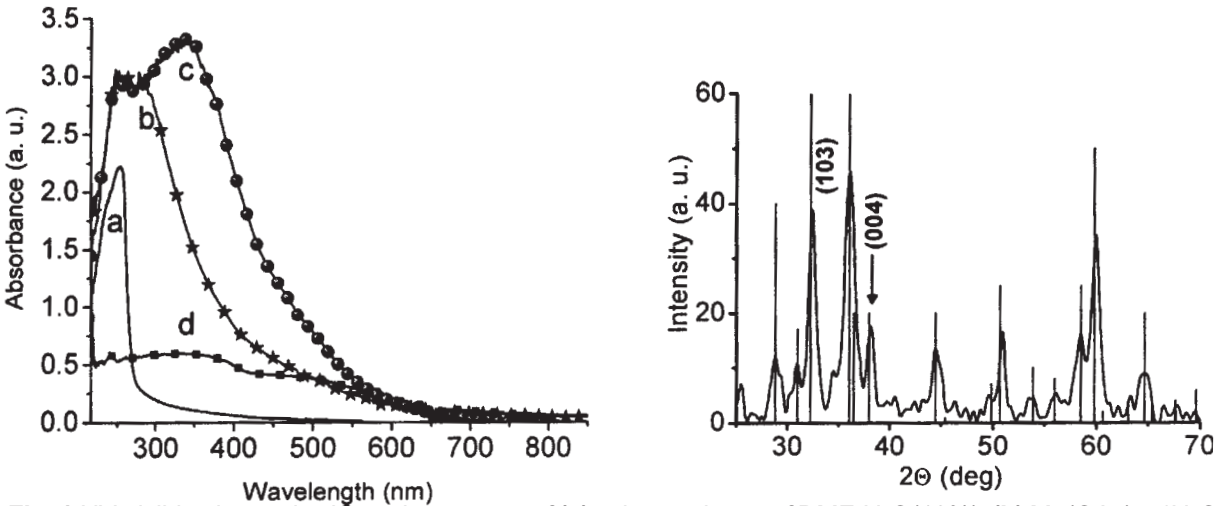

Fig. 1.UV-visible electronic absorption spectra of **(a)** solvent mixture of DMF-H_2O(10%), **(b)** $Mn(OAc)_2 \cdot 4H_2O$ $5 \cdot 10^{-3}$M immediately after dissolved and **(c)** one week later. This spectrum remains unchanged for 3 months, up to the time when Mn_3O_4 hausmannite precipitates as brown powder. **(d)** Absorption spectrum of the powder sample. Right, XRD pattern of Mn_3O_4 nanoparticles. The labeled peaks were used to determine the average crystallite size. All peaks can be indexed to Mn_3O_4 hausmannite, JCPDS # 24-0734.

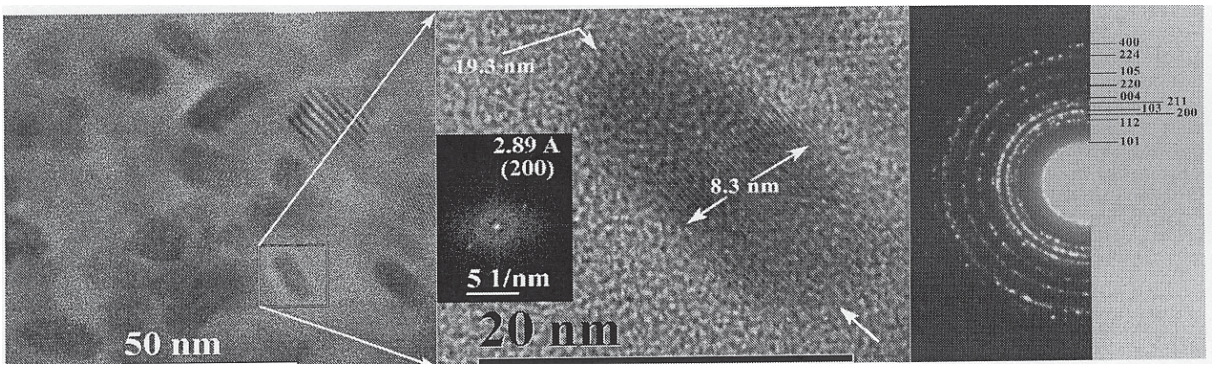

Fig. 2. HR-TEM micrographs of the Mn_3O_4 nanorods. Right, the corresponding electron diffraction pattern.

$Mn(OAc)_2 \cdot 4H_2O$ in DMF-H_2O(10%), exhibits a wide absorption band with an onset at 440 nm, one week later, this band becomes wider and the onset shifts to 558 nm. The spectrum remains unchanged after three months, time when the Mn_3O_4 precipitates as a brown fine powder. The electronic absorption spectrum of the precipitate obtained by diffuse reflectance measurement shows three well defined regions, one going from 250 to 410 nm, another from 410 to 585 nm and the last one finishing at 810 nm. The first portion is attributed to the allowed $O^{2-} \rightarrow Mn^{2+}$ and $O^{2-} \rightarrow Mn^{3+}$charge transfer transitions, and the last two can be reasonably related to d-d crystal field transitions. This spectrum is similar to the one published by J. Boyero *et al*. for the hausmannite phase [8].

The X-ray powder diffraction pattern (Fig. 1, right) reveals the formation of a nanosized Mn_3O_4 haussmanite. All diffraction peaks can be perfectly indexed to the hausmannite structure (JCPDS card 24-0734). The average crystallite size, 20.9 ± 0.19 nm, was calculated from the peak broadening, using the classical Scherrer-Warren equation over the (004) and (103) reflections. The relative intensity for the {00l} reflections is twice the reported values, which reveals a preferential orientation of nanocrystals along of <001> direction.

The precipitate also was analyzed by FTIR spectroscopy from 4000 to 400 cm^{-1}. The spectrum shows the characteristic absorption bands of νMn-O vibrations at 639, 532 and 409 cm^{-1}, this spectrum was consistent with that reported for Mn_3O_4 [4,8,9].

On the other hand, TEM micrograph obtained from a Mn_3O_4 colloidal dispersion sample, allowed us to confirm a preferential growth of the Mn_3O_4 nanostructures. The particle size distribution was determined over 100 nanoparticles, being the average diameter 6.5 ± 1.2 nm and the average length, 17.4 ± 4.1 nm, respectively. The average particle size, obtained from XRD pattern is in agreement with the observed average length.

HRTEM micrographs also corroborate the presence of elongated nanocrystals with dimensions close to those determined by X-ray and TEM experiments. A representative single elongated nanocrystal with a dimension of 8.3 nm x 19.3 nm can be observed in Fig. 2. The interplanar spacing of 2.89 Å corresponds to the (200) plane of tetragonal Mn_3O_4. In addition, the electron diffraction pattern confirms the nanorods to be composed of Mn_3O_4.

Q.Yitai *et. al*. [17] informed their prepared nanorods oriented to be oriented perpendicularly to the normal direction (101) to lattice planes, this direction being one of the natural growing axes for hausmannite. However, in the present case it is noteworthy that the rods are oriented with an axial direction parallel to the <001> zone axis.

A possible explanation of the morphology of Mn_3O_4 nanoparticles, obtained under the present reaction conditions, it may be that the growth of the {101} nanocrystals plane faces depends on the availability of Mn^{3+}, which in turn depends on the oxidation of Mn^{2+}. The growth along the <001> direction would be favoured by the fact that the density of Mn^{3+} in the (001) faces is lower than in the natural expected growing direction (e.g. <110>).

3.2. Magnetic Study

In bulk and monocrystal, Mn_3O_4 hausmannite is ferrimagnetic with a Curie temperature of about 42K

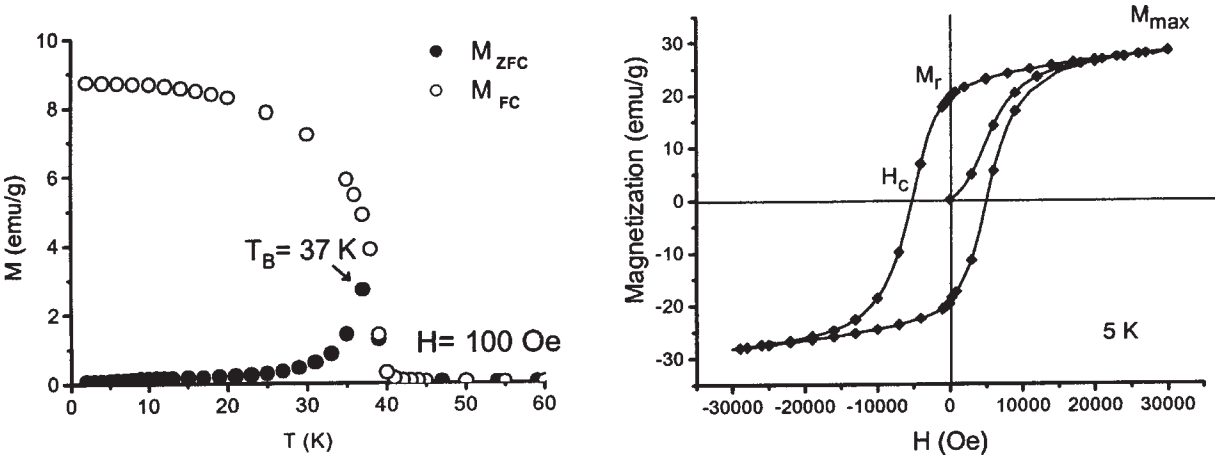

Fig. 3. Zero field cooled (ZFC) and field cooled (FC) magnetization curves of Mn_3O_4 nanorods under an applied field of 100 Oe (left). Hysteresis loop at 5K (right).

[18-20]. The Mn_3O_4 nanorods sample shows a ferrimagnetic behaviour at low temperature, and it is paramagnetic at room temperature. In the ZFC measurement, the sample was cooled from room temperature to 2K in absence of external magnetic field. Then, a magnetic field of 100 Oe was applied, and the magnetization of the sample was measured. When the temperature approaches 37K, the magnetization reaches a maximum and then starts to decrease. The temperature, at which the thermal activation overcomes all the energy barriers, is known as blocking temperature, T_B [21, 22] (Fig. 3). This result is similar to that reported by J. T. Park *et. al.* [23] for Mn_3O_4 spherical nanoparticles of 6 nm. Moreover, in the FC measurement, the sample was initially cooled to 2K under an applied magnetic field of 100 Oe. The subsequent magnetization measurement was recorded from 2 to 300K with the magnetic field kept at 100 Oe. The FC measurement showed a Curie temperature of 40K.

Although the hysteresis loop was obtained at 5K in a magnetic field of up to ± 30 kOe (Fig. 3), the saturation magnetization (M_s) was not reached, showing a maximum of magnetization (M_{max}) at about 26 emu/g, this value represents the 68.4% of the saturation magnetization in the bulk (M_S Mn_3O_4 = 38 emu/g) [24]. A remanence ratio (M_r/M_{max}) of 0.77 was estimated from the remanence value (M_r) of 20 emu/g. The coercivity (H_c) for these nanorods was of 5.2 kOe.

As expected, the magnetic behavior is under the influence of rods size. A principal effect of finite size is the breaking of a large number of bonds on the surface. Then the surface cations, produce a core of aligned spins surrounded by a disordered shell. This can result in a disordered spin configuration near to the surface and a reduced average net moment compared to the bulk materials. In addition, the surface spin states can result in high field hysteresis and relaxation of the magnetization [25], as have been observed for these nanorods.

3.3 Proposed reaction scheme

In general, the preparation of metal oxides requires a basic medium, and usually NaOH or LiOH are employed [26].

However, in this work the solvent mixture generates the basic medium, due to a hydrolysis mechanism [15].

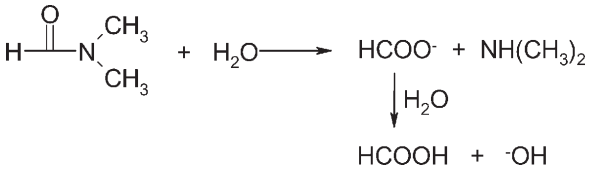

Besides, the acetate anions are involved in another hydrolysis equilibrium:

$CH_3COO^- + H_2O \rightarrow CH_3COOH + {}^-OH$

Therefore, the medium is basic enough to drive the formation of $Mn(OH)_2$, which is later oxidized to Mn_3O_4 with a simultaneous reduction of atmospheric oxygen. It is noteworthy that manganese nanoparticles are 30 times more efficient at promoting the manganese oxidation reaction than the bulk material [27].

$Mn^{2+} + 2^-OH \rightarrow Mn(OH)_2$ (Initiation)

$3Mn(OH)_2 + 1/2O_2 \rightarrow Mn_3O_4 + H_2O$
(Redox-condensation process)

Finally, this redox process makes the hausmannite to be the most stable product. The reaction sequence can be resumed as:

$$3Mn(OAc)_2 + 1/2O_2 \xrightarrow{DMF\text{-}H_2O(10\%)} \underset{\text{nanorods}}{Mn_3O_4} + 3H_2O$$

4. CONCLUSIONS

We have demonstrated that the dissolution of manganese(II) acetate in a mixture of polar solvents DMF-H_2O(10%) at room temperature, can be employed to obtain Mn_3O_4 nanoparticles in one step. These nanocrystals have an elongated morphology (rod-like shape) with a preferential orientation along <001> direction. The magnetic behavior is under the influence of rods size, showing high values of remanence ratio and coercivity. It is important to note that this novel synthesis method is clean, reproducible and requires neither complex apparatus and sophisticated techniques nor templates, and can be extended to other transition metal acetates in order to obtain different metal oxides. This possibility are currently investigated in our laboratory.

ACKNOWLEDGEMENTS

The support of this research by the CONACyT project J36514-E is gratefully acknowledged. We would like to thanks David Morales-Morales and Professor Jose Fripiat for their valuable comments.

REFERENCES

[1] O.Y. Gorbenko, I.E. Graboy, V.A. Amelichev, A.A. Bosak, A.R. Kaul, B. Guttler, V.L. Svetchnikov and H.W. Zandbergen // *Solid State Commun.* **124** (2002**)** 15.
[2] W. Zang, Z. Yang, Y. Liu, S. Tang, X. Han and M. Chen // *J. Cryst.Growth* **263** (2004) 394.
[3] G. Zhou, F. Rong, C. Xian-Hui and W. Yi-Cheng // *Inorg. Chem. Commun.* **4** (2001) 294.
[4] Z. Weixin, W. Cheng, Z. Xiaoming, X. Yi and Q. Yitai // *Solid State Ionics* **117** (1999) 331.
[5] W. Wang, C. Xu, G. Wang, Y. Liu and C. Zheng //*Adv. Mater.* **14** (2002) 837.
[6] S. Fritsch, J. Sarrias, A. Rousset and G.U. Kulkarni // *Mater. Res. Bull.* **33** (1998**)** 1185.
[7] V. Berbenni and V. Marini // *Mater. Res. Bull.* **38** (2003) 1859.
[8] J.M. Boyero, E.L. Fernandez, J.M. Gallardo-Amores, R.C. Ruano, V.E. Sanchez and E.B. Perez // *Int. J. Inorg. Mater.* **3** (2001) 889.
[9] F.A. Al Sagheer, M.A. Hasan, L. Pasupulety and M.I. Kaki // *J. Mater. Sci. Lett.* **18 (**1999) 209.
[10] E.R. Stobbe, B.A. de Boer and J.W. Geus // *Catal. Today* **47** (1999) 161.
[11] A. Vazquez-Olmos, D. Diaz, G. Rodriguez-Gattorno and J.M. Saniger-Blesa // *Colloid Polym. Sci.* **282** (2004) 957.
[12] J. Nemeth, G. Rodriguez-Gattorno, A.R. Vazquez-Olmos, D. Diaz and I. Dekany // *Langmuir* **20** (2004) 2855.
[13] G. Rodriguez-Gattorno, P. Santiago-Jacinto, L. Rendon-Vazquez, J. Nemeth, I. Dekany and D. Diaz // *J. Phys. Chem. B* **107** (2003) 12597.
[14] G. Rodriguez-Gattorno, D. Diaz, L. Rendon and G.O. Hernandez-Segura // *J. Phys. Chem. B* **106** (2002) 2482.
[15] R.V. Kumar, Y. Diamant and A. Gedanken // *Chem. Mater.* **12** (2000) 2301.
[16] I. Pastoriza-Santos andL.M. Liz-Marzan // *Pure Appl. Chem.* **72** (2000) 83.
[17] B. Yang, H. Hu, C. Li, X. Yang, Q. Li and Y. Qian // *Chem. Lett.* **33** (2004) 804.
[18] K. Dwight and N. Menyuk // *Phys. Rev.* **119**, (1960) 1470.
[19] C.B. Azzoni, M.C. Mozzati, L. Malavasi, P. Ghigna and G. Flor // *Solid State Commun.* **119** (2001) 591.
[20] Y.Q. Chang, X.Y. Xu, X.H. Luo, C.P. Chen and D.P. Yu // *J. Cryst. Growth* **264** (2004) 232.
[21] A.J. Rondinone, A.C.S. Samia and Z.J. Zhang // *J. Phys. Chem. B* **103** (1999) 6876.
[22] J. Garcia-Otero, M. Porto, J. Rivas and A. Bunde // *Phys. Rev. Lett.* **84** (2000) 167.
[23] W.S. Seo, H.H. Joe, B. Kim and J.T. Park // Angew. Chem. Int. Ed. **43** (2004) 1115.
[24] R.S. Tebble and D.J. Craik, *Magnetic Materials* (New York, 1969).
[25] R.H. Kodama // *J. Magn. Magn. Mater.* **200** (1999) 359.
[26] V.G. Kumar, D. Aurbuch and A. Gedanken // *Ultrason. Sonochem.* **10** (2003**)** 17.
[27] M.F. Hochella, C.J. Tadanier, S.K. Lower, B.H. Lower, T.A. Kendall, T.A. Cail and A.S. Madden // *Geochim. Cosmochim. Acta* **67 (**2003) A153.